

A LINEAR 3-D FINITE ELEMENT UNIT CELL MODEL FOR FIBRE WAVINESS IN COMPOSITE MATERIALS

Andrew J. Gunnion^a, Murray L. Scott^a, Rodney S. Thomson^b and Dieter Hachenberg^c

^a The Sir Lawrence Wackett Centre for Aerospace Design Technology
Department of Aerospace Engineering, RMIT University
GPO Box 2476V, Melbourne, Victoria 3001, Australia

^b Cooperative Research Centre for Advanced Composite Structures Limited
506 Lorimer Street, Fishermans Bend, Victoria 3207, Australia

^c Airbus Deutschland GmbH
Kreetslag 10, 21129 Hamburg, Germany

Keywords: *fibre waviness, finite element, voxel, composite materials*

Abstract

Composite materials have great potential to continue to improve the efficiency of aircraft manufacture and operation, however they are still limited in their applications because of their damage tolerance properties. As a result, the damage tolerance of composites is still being extensively researched around the world. The purpose of such research is to gain understanding of failure mechanisms and develop improved failure models, hopefully reducing conservative design factors. Researchers are also improving the damage tolerance of composite materials by such methods as toughened resins or through-thickness reinforcement (TTR).

The development of a simple unit cell model to investigate the mechanical properties of a composite laminate with TTR is presented. The equivalent stiffness of the unit cell is evaluated using a voxel (volume pixel), finite element (FE) model. The model results are compared to literature and prove to offer equivalent or better results, at a quarter of the required elements, reducing time and resources required for analysis. The model developed will continue to be further refined and validated using experimental results.

1 Introduction

The need for safer, cheaper and better performing aircraft continues to propel developments in advanced materials and manufacturing techniques. Composite materials have the potential to improve on existing structure, but have been limited by their damage tolerance properties.

In an effort to improve existing aircraft design, extensive research is underway to understand the failure mechanisms of composite materials, and to improve their damage tolerance. Laminate reinforcement by stitching or Z-pinning, is one method of improving damage tolerance that is under investigation [1-12]. Stitching of dry preforms also offers additional advantages of reduced part count and possibly lowering manufacture costs [3]. However, whilst the addition of TTR has been well documented to improve damage tolerance in composite laminates, it comes at a cost to in-plane strength and stiffness [1-6,9,13-14]. Extensive experimental work has been performed to characterise many aspects of stitched composite properties [4,7-8,11-15]. For a thorough review of TTR, several comprehensive review articles have already been published [1,3,14].

Fibre misalignment or fibre waviness result as the fibres are pushed aside to accommodate the reinforcement [5]. Fibre waviness may also form as a consequence of the manufacturing process, particularly in thick cross-ply laminates or in filament wound structures [16].

Whether the compromise between damage tolerance and mechanical properties warrants the use of TTR depends on many design considerations. To aid the designer in making such decisions, the ability to accurately predict the impact of TTR in a composite laminate is essential.

Many models, linear [16-21] and nonlinear [22-26], exist for investigating the behaviour of undulating fibres, using analytical [18-24] and FE approaches [25-26]. Likewise, many models have been proposed for the behaviour of a laminate with TTR, using micromechanics, laminate theory and FE methods [6] for calculation.

In this paper, a simple linear unit cell model is presented for the prediction of properties of a reinforced laminate with consequential in-plane fibre waviness. The geometry is represented by voxels; that is, as discrete volume blocks, instead of modelling the geometry as a continuum. This method of modelling lends itself well to FE analysis, as well as the stiffness averaging calculation methods. The voxel modelling approach is advantageous because it is easily automated, allows rapid model adjustments and it guarantees mesh compatibility if multiple stacked plies are investigated.

2 Unit Cell Models

2.1 Model Assumptions

In order to reduce the complexity of the geometry and model detail to a manageable scale, the following assumptions were made with reference to Figure 1:

- The stitching threads are assumed to be a singular, cylindrical body orientated perpendicular to the laminar plane.

- Thread primary modulus is aligned in the thread direction, giving thread transverse properties in the laminate plane.
- The fibre misalignment is sinusoidal around the TTR.
- Within the fibre region, the volume fraction and material properties are assumed to be that of the unstitched laminate, prior to misalignment.
- Regions of pure resin exist either side of the reinforcement and are assumed to be isotropic.
- The reinforcement and ply fibres are assumed to be orthotropic.
- Fibre crimpage (out-of-plane waviness) as a result of the stitching process in the outer most plies is ignored.
- Fibres are assumed to have maximum undulation along the line of stitching, and the waviness amplitude fades linearly to zero at some defined distance, y_t , from the TTR. The spread of further waviness caused by the displacement of adjacent fibres is controlled with an input variable.

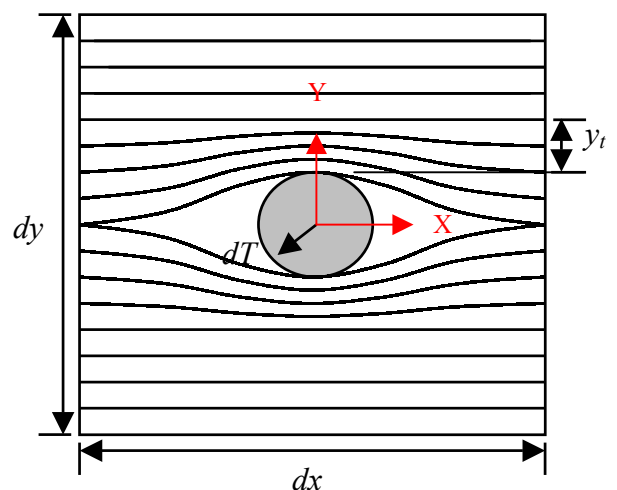


Fig. 1. Graded waviness TTR unit cell model.

Where:

- dx unit cell length in x direction.
- dy unit cell width in y direction.
- dT TTR radius.
- y_t Transition distance, over which waviness fades to zero. $0 \leq y_t \leq dy/2$

If the stitching direction matches the ply direction, dx is equal to the stitch pitch, and dy the row spacing. If the stitch direction is orthogonal to the longitudinal ply direction, then dx is equal to the row spacing and dy the stitch pitch.

Given the above terms and local ply coordinate system shown in Figure 1, the automated modelling tool determines the material and groups each element according to the conditions outlined in Table 1.

Table 1. Boundary Description of Material Regions.

Material	Condition
Undisturbed Fibres	$dT + y_i < y$
TTR	$\sqrt{x^2 + y^2} \leq dT$
Matrix	$\sqrt{dT^2 - x^2} < y \leq \frac{dT}{2} \left(\cos\left(\frac{2\pi x}{dx}\right) + 1 \right)$
Misaligned Fibres	$\frac{dT}{2} \left(\cos\left(\frac{2\pi x}{dx}\right) + 1 \right) < y \leq dT + y_i$

Where fibres are deemed misaligned, their misalignment angle, α , from the local ply orientation, θ , is given by Equation 1. This function governs the fading of waviness and the sign of the misalignment angle.

$$\alpha = \left(\frac{y}{|y|} \right) \left(\frac{dT + y_i - |y|}{dT + y_i} \right) \tan^{-1} \left(\frac{dT\pi}{dx} \left(1 - \sin\left(\frac{2\pi x}{dx}\right) \right) \right) \quad (1)$$

2.2 Unit Cell Types

The graded waviness unit cell is a full repeating and symmetric unit cell, meaning that the laminate can be constructed by tiling unit cells with uniform orientation, or by reflecting along any of its boundaries. This is important for the application of boundary conditions.

3 Boundary Conditions

In order to extract equivalent laminate properties from the unit cell models, boundary conditions must be applied in such a way that the unit cell behaves as though other identical unit cells surround it. The calculation requires

the computation of six separate iso-strain load cases. Each load case requires a specific set of boundary conditions be applied to ensure correct periodicity is maintained. The iso-strain load cases and boundary conditions used were based on those available in literature [27].

To minimise modelling time, a software tool was written where all the major model parameters and material properties are inputted, and the 3-D model is automatically generated. Boundary conditions and load cases are defined as part of the automated process, leaving the user with no further role after inputting the model parameters until the results are to be processed.

Whilst the pure tensile load cases are relatively simple to model, shear boundary conditions can be difficult to capture accurately [28]. Implementing boundary conditions for the three shear iso-strain boundary conditions required additional attention to ensure that periodic requirements were correctly satisfied. An isotropic, homogeneous unit cell under iso-strain shear boundary conditions will deform with straight boundaries. However, this is not the case for a heterogeneous unit cell, as shown in Figure 2. Note that whilst the boundaries of the sheared unit cell are not linear, they are periodic, satisfying the important boundary condition for unit cell analysis. This can be confirmed by examining the behaviour of a unit cell surrounded by identical unit cells along all boundaries [28].

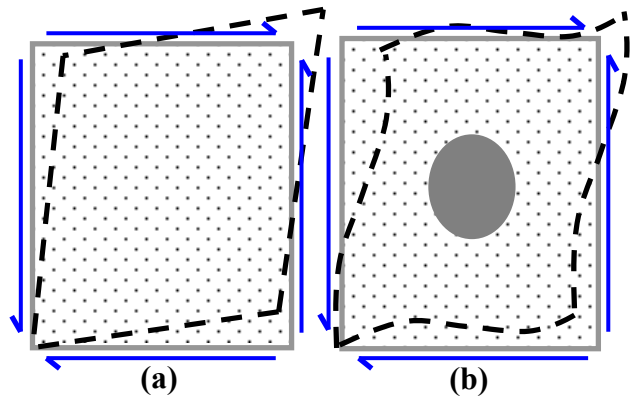


Fig. 2. Shear boundary deformation for a) isotropic, homogeneous unit cell, b) anisotropic, heterogeneous unit cell.

Previous studies have applied shear boundary conditions that constrain boundaries to remain straight [6]. Such over-constraint yields higher shear modulus results. Periodic boundary conditions yield theoretically correct shear results, however the final properties must still be viewed with an appropriate level of caution, given the complex shear behaviour of a composite laminate.

Figure 3 shows the exaggerated deformation in the voxel model resulting from correct iso-strain shear boundary conditions in the x - y plane. It can be seen that the unit cell remains periodic even though the boundaries are curved.

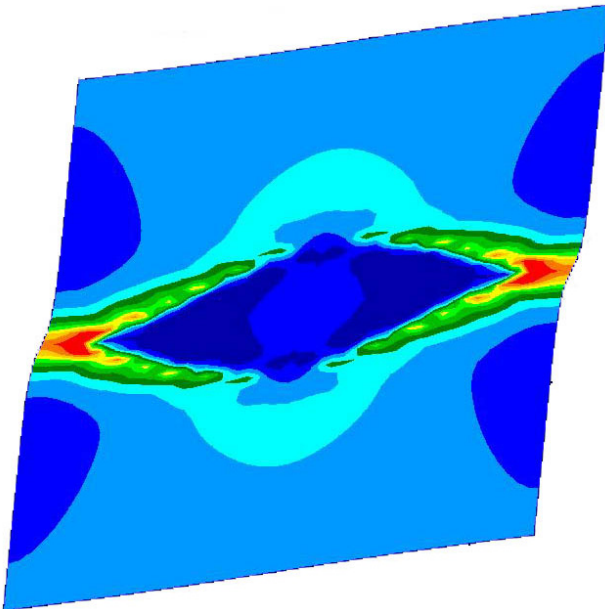


Fig. 3. Exaggerated boundary deformation resulting from iso-strain shear BCs. Colours indicate shear stress pattern within the strained unit cell.

4 Voxel Approach

4.1 Concept

In FE analysis, it is typical to define the geometry of the subject, and then generate a mesh that adheres to the specified geometric confines. Alternatively, a voxel model approach can be adopted, where limiting mesh size and shape approximates the geometry of the subject. A voxel model, made from many voxels, is analogous to a picture made of many pixels. The quality of the approximation is

therefore dependant on the size, or resolution of the voxel model, and the purpose of the analysis. Stiffness prediction by FE methods involves volumetric averaging of the stresses within the model. Such analysis is well suited to a voxel approach because the effect of localised stress concentrations along jagged boundaries is insignificant when averaged across the entire body.

4.2 Model Automation

Adopting a voxel approach makes model automation a simpler task. For the TTR unit cell models presented, a *blank solid* is first created and meshed at the desired resolution. It is important that the mesh size be small enough to accurately represent all unit cell constituents in their correct volume fractions. The software tool then scans through the elements, determining their material properties and orientation based on the element coordinates and a mathematical description of the geometry, see Table 1 and Equation 1. Elements are then grouped by type to allow simple visual representation of the model with the use of colours. This approach proves to be quick and there is no need to examine the mesh for poor element topologies as a result of meshing complex geometric regions. A resulting model is shown in Figure 4, where plies of different orientations are assigned different colours for clarity. The modelling tool was programmed in Patran Command Language (PCL) to operate in the Patran environment using Nastran as the FE solver.

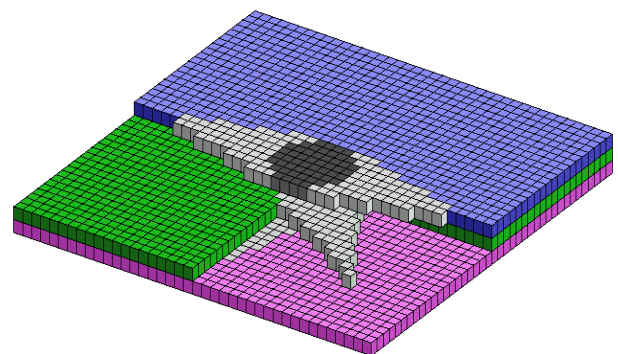


Figure 4. 3-D cut-away image of voxel model with 0° (blue), 45° (green) and 90° (pink) plies, TTR (dark grey) and resin regions (light grey) clearly indicated.

The voxel approach also solves the difficult problem of mesh compatibility between two adjacent plies in the analysis of a laminate, as seen in Figure 5. If two orthogonal adjacent plies were meshed strictly according to their geometric boundaries, the two meshed plies will not be compatible when stacked. This problem is worsened with the addition of +45/-45 plies. Hinders and Dickinson [6] adopt a star like arrangement, where in one ply, the unit cell geometry is rotated in 0/90/45/-45 orientations, and the resulting star shape is meshed. This ensures compatibility across plies of different orientations; however generating the mesh without distorted elements is difficult. The resulting mesh, which must be redefined for different unit cell geometries, requires three to four thousand solid elements per ply.

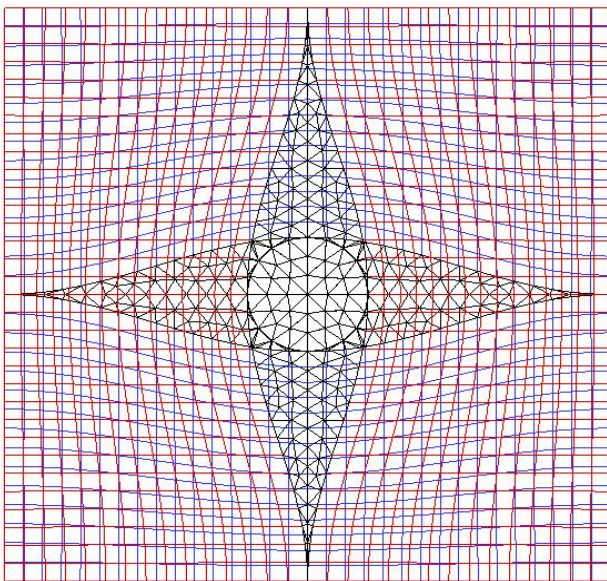
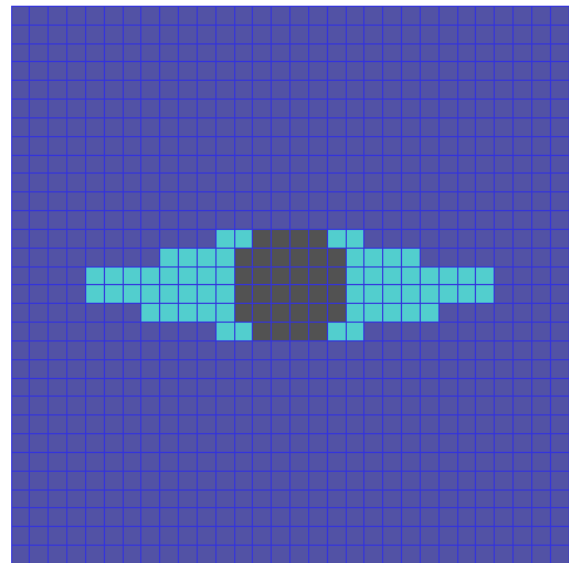


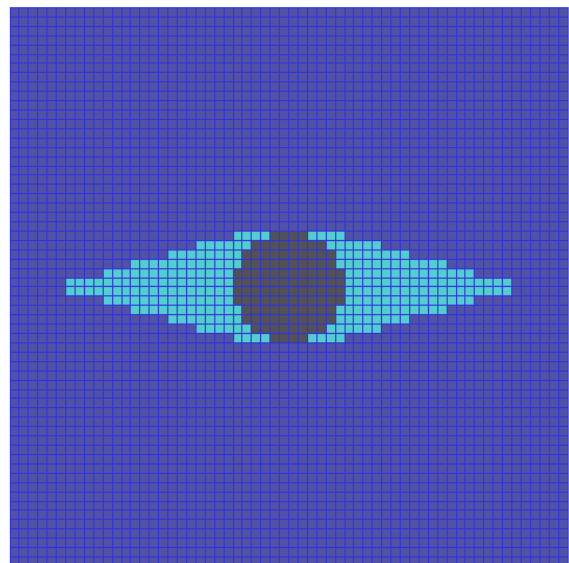
Fig. 5. Mesh mismatch that arises from stacking of conventionally meshed unit cells.

4.3 Mesh Size Investigation

It has been mentioned that the accuracy of the result is dependant upon the size of the mesh used to construct the voxel model. Two methods to gauge if the mesh size is sufficiently small are to compare the results to a conventionally meshed model, or to systematically refine the mesh size until the results converge.



(a)



(b)

Fig. 6. Voxel unit cell models, (a) 900 Elements, 30 x 30, (b) 3600 Elements, 60 x 60.

To determine a satisfactory mesh size for the proposed unit cell model, results were compared at different mesh sizes to a conventionally meshed unit cell, for two different reinforcement volume fractions. Table 2 shows the primary Young's Modulus (E_1) calculated at different mesh resolutions normalized to the conventional mesh model for two different reinforcement diameters. Mesh sizes of 30 x 30 and 60 x 60 were used, and are shown in Figure 6 (a) and (b).

It can be seen from Table 2 that the improvement in results is less than 0.5%, but requires four times as many elements. Therefore, a mesh grid of 30 x 30 elements per ply was adopted for the final analyses.

Table 2. Primary Young's Modulus (E_1) voxel results normalised to conventional mesh.

	900 Elements 30 x 30	3600 Elements 60 x 60
TTR $V_f = 3\%$	0.995	0.997
TTR $V_f = 6\%$	0.995	0.998

6 Model Comparison

The results of the voxel model were compared to similar results available in the literature. Hinders and Dickinson compared their FE unit cell model to results computed by the software Texcad [6]. Texcad uses orientation averaging under isostrain conditions to evaluate unit cells [29]. The models chosen for comparison are summarised in Table 3, and material properties are given in Table 4.

Table 3. Summary of models compared.

Series Name	TTR Material	TTR V_f	Layup
c4a	C/ep	0.3 %	[0/90]
c2a	C/ep	1.9 %	[0/90]
c5a	Gr/ep	4.9 %	[0/90]
c2a-kev	Kevlar	1.9 %	[0/90]
c2a-ti	Titanium	1.9 %	[0/90]
c2a-steel	Steel	1.9 %	[0/90]
c2b	Gr/ep	1.9 %	[+45/-45]
c2c	Gr/ep	1.9 %	[0/0]
c2quasi	Gr/ep	1.9 %	[45/0/-45/90]

Table 4. Summary of investigated materials.

Material	E_1 (GPa)	E_2 (GPa)	G_{12} (GPa)	G_{23} (GPa)	V_{12}
Lamina AS4/3501-6	134	8.69	5.84	3.15	0.25
TTR T300/9310	141	7.17	4.37	2.61	0.25
TTR Kev/3501-6	38.6	8.96	5.48	5.27	0.31
TTR Titanium	110	-	43.4	-	0.30
TTR Steel	207	-	82.7	-	0.28
Resin 3501-6	4.36	-	1.62	-	0.34

For complete listing of all model variables, see ref. [6].

7 Results

Figures 7 through 9 plot E_1 for all analysed models compared to the reference FE and Texcad solutions [6]. The annotations refer to the percentage difference between the voxel and reference FE solution. Similarly, Figures 10 through 12 plot G_{12} for all analysed models compared to the reference solutions.

Figure 13 shows E_1 , E_2 and E_3 for a unidirectional (UD) laminate and a quasi-isotropic laminate normalised to the unstitched modulus versus volume fraction percentage of TTR. Data are plotted to a TTR V_f of 10%, though typically in practice reinforcement does not exceed roughly 5%.

8 Discussion

From Figures 7 through 9 it can be seen that the E_1 calculated with the voxel model is very similar, though slightly less than that from the literature. The average difference was only 2.8%, with a maximum of 8.9% between the voxel and reference FE solution. This is explained by differences in the unit cell model and not the mesh methodology. Hinders et al. [6] assume a smaller region of fibre misalignment, and that the angle is constant. This model presented assumes a sinusoidal fibre misalignment, and is not able to confine the waviness to the small bands assumed by Hinders et al. [6].

Similarly, the shear modulus determined by the voxel model was always lower than that of the other methods, typically the difference was around 4%, however where 45° plies were present in the laminate, this difference increased up to 17%. This difference can be explained by the different boundary condition methods for the shear iso-strain load cases. The reference solution requires that boundaries remain straight, resulting in a slightly stiffer shear modulus. The larger difference in shear results for laminates with 45° plies suggests that such

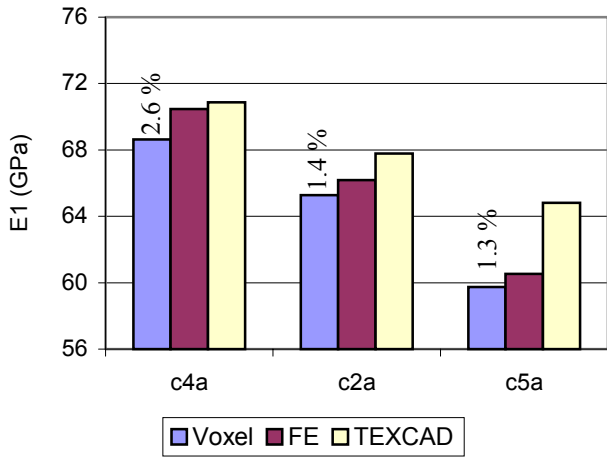


Fig. 7. E_1 for models with decreasing TTR V_f .

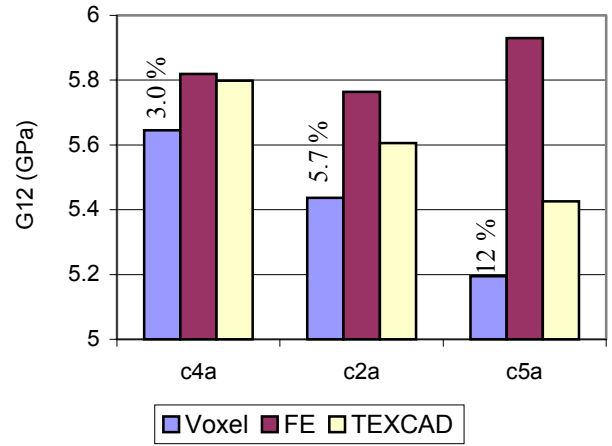


Fig. 10. G_{12} for models with decreasing TTR V_f .

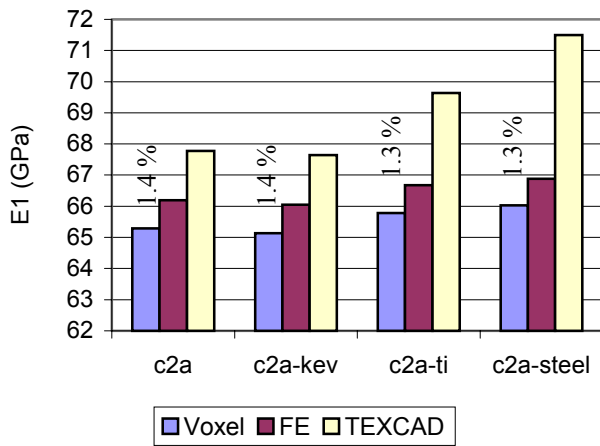


Fig. 8. E_1 increases with TTR stiffness. $V_f = 1.9\%$.

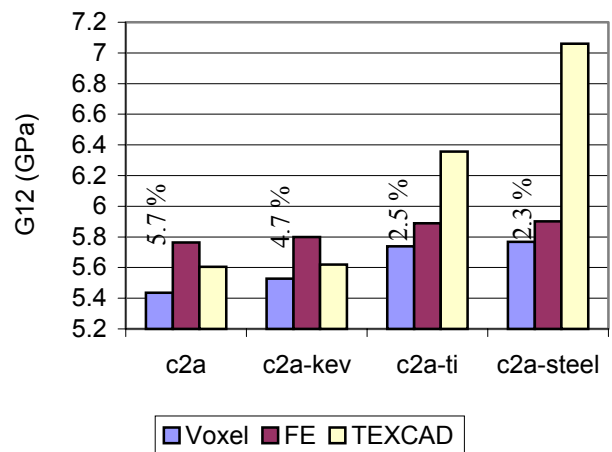


Fig. 11. G_{12} increases with TTR stiffness. $V_f = 1.9\%$.

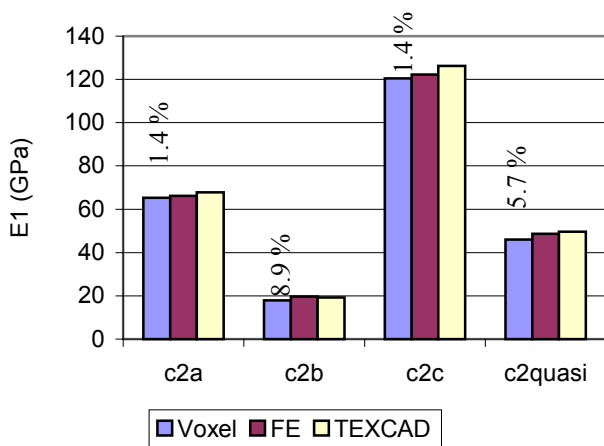


Fig. 9. E_1 is strongly dependent on laminate design.

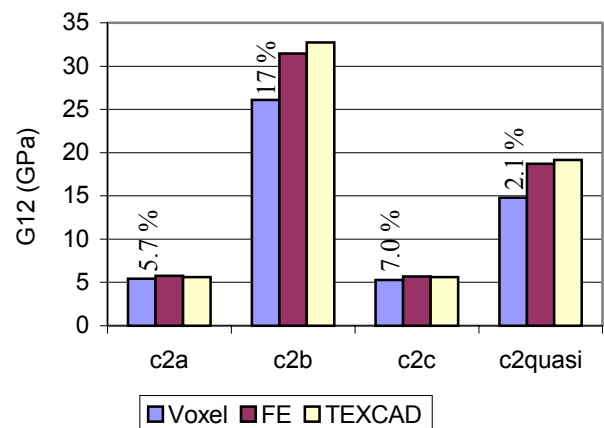


Fig. 12. G_{12} is strongly dependent on laminate design.

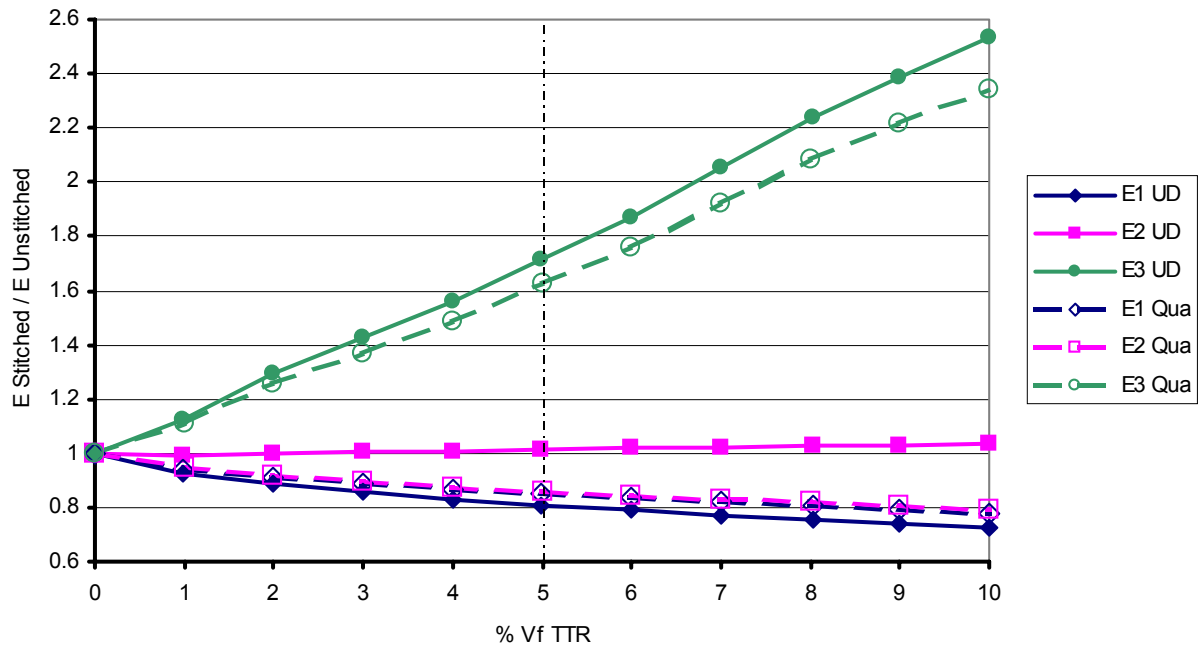


Fig. 13. Normalised E_1 , E_2 and E_3 of a UD and quasi-isotropic laminate versus %Vf of TTR.

cells deform with more significant distortion of the cell boundaries.

In addition to comparing analysis methods, the figures also provide insight into the effect of major parameters on the resulting stiffness. Figures 7 and 10 show a decrease in Young's Modulus and Shear Modulus as the volume of reinforcement increases. The reference shear result for c5a in Figure 10 is somewhat erroneous in light of the voxel, Texcad and other FE results and is therefore questionable.

Figures 8 and 11 depict a general trend in calculated response of a reinforced laminate for the in-plane properties to increase with an increase in reinforcement material stiffness. However, the overall change as a result of changing reinforcement material remains quite small as a percentage of overall stiffness. Selection of a reinforcement material is therefore driven by other factors such as manufacturing method, cost, etc.

Figures 9 and 12 plot the effect of TTR on different laminates. It is expected that the reduction in laminate stiffness resulting from TTR is more significant where plies are oriented in the loading direction. The more significant percentage variation shown in Figure 9 than Figures 7 and 8 is a mathematical consequence

of relatively low modulus models and not an inadequacy in the modelling procedure.

Figure 13 shows that the in-plane properties are reduced as a consequence of TTR, and that the decrease continues with an increase in TTR. For a unidirectional laminate, the decrease is more significant than that of a quasi-isotropic laminate. The effect of stitching on E_2 of a unidirectional laminate was negligible, because the transverse modulus is significantly lower than that in the fibre direction, and is not greatly influenced by fibre misalignment. The out of plane modulus, E_3 , rose significantly with an increase in TTR. This is an expected result as the amount of fibres in the out-of-plane direction increases with stitching; the rate of increase of E_3 is more significant than the decrease in E_1 and E_2 . The magnitude of reduction in in-plane properties is inline with expectations highlighted in a compilation of experimental data [9].

9 Conclusion

A voxel based, finite element unit cell model has been presented for calculating effective mechanical properties of a through-thickness reinforced laminate. The voxel method is advantageous for this type of analysis because it

allows fast, automated pre- and post-processing, guarantees mesh compatibility between adjacent plies in a laminate analysis, and is capable of giving satisfactory results with fewer elements.

The voxel model results were compared to a reference FE solution. Young's Modulus results were typically within 1.4% of the reference FE solution, however a couple of larger variations brought the average to 2.9% variation. Larger variation was found when comparing shear modulus results, an average of 8.4%, however this can be attributed to differences in boundary condition assumptions. The models were generated using a simple-to-use, automated software tool currently under further development. The models were computed using approximately one quarter of the elements used in the reference results, proving the validity of the voxel approach as an efficient method to determine equivalent linear stiffness properties.

Investigating the effects of stitching on both unidirectional and quasi-isotropic laminates using the voxel model reveals a decrease in in-plane properties and significant increase in out-of-plane stiffness with an increase in reinforcement. This result is inline with expectations from experimental data.

Acknowledgements

The authors would like to acknowledge the support of the Cooperative Research Centre for Advanced Composite Structures Ltd, Airbus Deutschland GmbH, and also the support through the Australian Postgraduate Awards Scheme.

References

- [1] Dickinson LC, Farley GL and Hinders MK. Translaminar Reinforced Composites: A Review. *Journal of Composites Technology & Research*, Vol 19, pp 3-15, 1997.
- [2] Dickinson LC, Farley GL and Hinders MK. Failure initiation in translaminar reinforced composites. *Journal of Composites Technology & Research*, Vol 22, pp 23-33, 2000.
- [3] Dransfield K, Baillie C and Mai YW. Improving the delamination resistance of CFRP composites with the use of through-thickness reinforcement – A Review. *CRC-AS TM 92007*, 1993.
- [4] Herszberg I and Bannister MK. Compression and Compression-After-Impact properties of thin stitched carbon/epoxy composites. *CRC-AS CP 93001*, Melbourne, 1993.
- [5] Herszberg I and Bannister MK. Tensile properties of thin stitched carbon/epoxy composites, *Proceedings 5th Australian Aeronautical Conference*, Melbourne, Australia, pp 213-218, 1993.
- [6] Hinders M and Dickinson L. Trans-Laminar-Reinforced (TLR) Composites. *NASA-CR-204196*, 1997.
- [7] Larsson F. Damage tolerance of a stitched carbon/epoxy laminate. *Composites: Part A*, pp 923-934, 1997.
- [8] Mouritz AP. The damage to stitched GRP laminates by underwater explosion shock loading. *Composites Science and Technology*, Vol 55, pp 365-374, 1995.
- [9] Mouritz AP and Cox BN. A mechanistic approach to the properties of stitched laminates. *Composites: Part A*, Vol 31, pp 1-27, 2000.
- [10] Mouritz AP, Gallagher J and Goodwin AA. Flexural strength and interlaminar shear strength of stitched GRP laminates following repeated impacts. *Composites Science and Technology*, Vol 57, pp 509-522, 1997.
- [11] Pelstring RM and Madan RC. Stitching to improve damage tolerance of composites. *34th International SAMPE Symposium*, May 8-11, Book 2 of 2, pp 1519-1528, 1989.
- [12] Rugg KL, Cox BN and Massabo R. Mixed mode delamination of polymer composite laminates reinforced through the thickness by z-fibers. *Composites: Part A*, Vol 33, pp 177-190, 2002.
- [13] Farley GL. A mechanism responsible for reducing compression strength of through-the-thickness reinforced composites. *Journal of Composite Materials*, Vol 26, pp.1784-1795, 1992.
- [14] Mouritz AP, Leong KH and Herszberg I. A review of the effect of stitching on the in-plane mechanical properties of fibre-reinforced polymer composites. *Composites: Part A*, Vol 28, pp 979-991, 1997.
- [15] Tanner ME and Adams DO. Analysis of damage development in stitched composite stiffeners. *31st International SAMPE Technical Conference*, October 26-30, pp 367-377, 1999.
- [16] Hsiao HM and Daniel IM. Effect of fiber waviness on stiffness and strength reduction of unidirectional composites under compressive loading. *Composites Science and Technology*, Vol 56, pp 581-593, 1996.
- [17] Chan WS and Chou CJ. Effects of delamination and ply fiber waviness on effective axial and bending stiffness in composite laminates. *Composite Structures*, Vol 30, pp 299-306, 1995.

- [18] Hsiao HM and Daniel IM. Elastic properties of composites with fiber waviness. *Composites Part A*, Vol 27, pp 931-941, 1996.
- [19] Piggott MR. The effect of fibre waviness on the mechanical properties of unidirectional fibre composites: A review. *Composites Science and Technology*, Vol 53, pp 201-205, 1995.
- [20] Telegadas HD and Hyer MW. The influence of layer waviness on the stress state in hydrostatically loaded cylinders: Failure Predictions. *Journal of Reinforced Plastics and Composites*, Vol 11, pp127-145, 1992.
- [21] Zhongming G and Dechao Z. Micromechanical analysis of the strength of fiber composites with unidirectional undulation. *APCSMS Proceedings*, Beijing, China, (A97-31093 08-39), pp. 307-311, 1996.
- [22] Bogetti T, Gillespie Jr JW and Lomontia MA. The influence of ply waviness with nonlinear shear on the stiffness and strength reduction of composite laminates. *Mechanics of Composite Materials: Nonlinear effects*, Vol 159, pp 163-172, 1993.
- [23] Chun H-J, Shin J-Y and Daniel IM. Effects of material and geometric nonlinearities on the tensile and compressive behaviour of composite materials with fiber waviness. *Composites Science and Technology*, Vol 61, pp125-134, 2001.
- [24] Rai HG, Rogers CW and Crane DA. Mechanics of curved fiber composites. *Journal of Reinforced Plastics and Composites*, Vol 11, pp 552-566, 1992.
- [25] Kyriakides S and Ruff AE. Aspects of the failure and postfailure of fiber composites in compression. *Journal of Composite Materials*, Vol 31, pp 2000-2037, 1997.
- [26] Wisnom MR. Modelling the effects of fibre waviness on compressive failure in unidirectional composites. *Composite Material Technology IV*, pp231-238, 1994.
- [27] Tan P, Tong L and Steven GP. Modeling Approaches for 3D orthogonal woven composites. *Journal of Reinforced Plastics and Composites*, Vol 17, No. 6, pp 545-577, 1998.
- [28] Sun CT and Vaidya RS. Prediction of composite properties from a representative volume element. *Composites Science and Technology*, Vol 56, pp 171-179, 1996.
- [29] Cox BN and Flanagan G. Handbook of analytical methods for textile composites. *NASA Contractor Report 4750*, 1997.